Effect of sensor shape on the equivalent impedance signature for the detection of defects using eddy current testing

Abdeslam Aoukili*

National School of Applied Sciences at Tetouan, Abdelmalek Essaadi University, Tetouan 93030, Morocco

Abstract. Eddy current testing is widely used for non-destructive evaluation of electrically conductive materials. This technique was recognized to be quite sensitive to defects affecting the geometry of a part or its electromagnetic properties, such as inclusions, cracks or corrosion. It is easy to implement, sturdy in the context of industrial applications and relatively inexpensive. Due to the growing need for reliability, the development of new eddy current systems is required. This work was dedicated to the design of new shapes of probes with the aim to increase detection capability. The objective is to assess how probe design can improve imperfection presence signature in a tested specimen. The methodology used is based on finite element simulation of B-scan process and calculation of the equivalent impedance seen across the terminals of the probe. Monitoring variations of this impedance for both the flawless control case and that with the presence of a defect was performed. Seven different shapes of probes were studied. It was found that the signature associated to the variation undergone by the impedance depends hugely on the probe geometry.

1 Introduction

Eddy Current Testing (ECT) is routinely employed to control the quality of conductive materials such as aluminum, copper, or steel. This method is part of general Non-Destructive Evaluation (NDE) techniques that are based on monitoring electromagnetic properties of inspected specimens [1]. These methods which enable detecting surface and subsurface damage incorporate two techniques: Magnetic Particle Inspection (MPI) and Eddy currents (EC) [2]. The latter approach is based on using electromagnetic induction to examine the presence of flaws in conductive materials, even if these have not ferromagnetic properties. Access to the surface of the inspected conductive part material must nevertheless be feasible. Also, the state surface finish of the part must be sufficiently flat in order to avoid superfluous disturbance of the signal. Considering EC technique under stationary excitation regime, it is well known that the penetration zone at the skin of the inspected part depends on the conductivity of the material as well as on the work frequency. These should be adequate to enable any detection. However, if the orientation of the tracked flaw direction goes far from being orthogonal to that of the probe this could not be sensed easily. Therefore, working to get better orientation of probe with respect to a potential flaw constitutes a matter of major import in the framework of this technique.

In common configuration of EC testing, an excitation coil with alternating current is positioned enough close to the tested part surface. Due to induction phenomenon, the current circulation in the coil creates a variable magnetic field. Now, interaction of this latter with the part material generates a current in a receiver coil. This signal detects any change of inductive magnetic flow. As many parameters intervene in the problem, simulation based approach has many advantages in the design of EC systems. This enables to resolve with cost-effectiveness the influence of factors on the sensor indication.

In this work, a numerical simulation of the electromagnetic field appearing in a perfectly conductive part is performed. The material of the inspected part is assumed to be homogeneous and isotropic. A harmonic induction field which is generated by a coil is applied as the excitation signal. Simulation of the inspection course is performed by using the finite element method under Comsol software. A small defect having the form of a parallelepiped cavity is inserted on the specimen surface and the B-scan procedure consisting of line sweeping is executed [3]. Detection is achieved by monitoring the variations disturbing the equivalent circuit impedance [4]. Various shapes of the sensing probe having the same volume are proposed. The effect of their geometry on the EC indicator signal is evaluated via monitoring their equivalent impedances as function of the distance separating the probe from the inserted defect in a plate.

2 Theory of EC based detection

The low-frequency approximation of the Maxwell equations for a linear conductive material domain is used in the following. The Maxwell equations write [5]

* Corresponding author: abdeslamaoukili@gmail.com

$$\vec{\nabla}.\vec{E} = \frac{\rho}{\varepsilon} \quad (1)$$

$$\vec{\nabla}.\vec{B} = 0 \quad (2)$$

$$\vec{\nabla} \times \vec{E} = -j\omega\vec{B} \quad (3)$$

$$\vec{\nabla} \times \vec{B} = \mu\vec{J}_{ext} + \mu(\sigma + j\omega\varepsilon)\vec{E} \quad (4)$$

where $\vec{E}$ is the electric field, $\vec{B}$ magnetic flux density, $\vec{J}_{ext}$ density of external sources applied current, ρ volumetric density of electric charge, ε permittivity of the medium, σ conductivity, μ permeability of the medium, ω the angular frequency, $\vec{\nabla}$ the nabla symbol and j the unit pure imaginary complex number.

To solve equations (1) to (4), the magnetic vector potential ($\vec{A}$) and the electric scalar potential (ϕ) are introduced. These are defined by:

$$\vec{B} = \vec{\nabla} \times \vec{A} \quad (5)$$

$$\vec{E} = -\vec{\nabla}\phi - j\omega\vec{A} \quad (6)$$

The EC approximation holds for metals for which $\omega\varepsilon << \sigma$ is satisfied in the low frequency regime (in general for a frequency that is less than $1MHz$). The problem can then be stated in terms of the magnetic vector potential by means of the following equation [6]:

$$\vec{\Delta}\vec{A} - j\mu\omega\sigma\vec{A} = -\mu\vec{J}_{ext} \quad (7)$$

where $\vec{\Delta}$ is the Laplace operator.

Eq. (7) is solved for a given domain with specified boundary conditions. The impedance of a coil which is placed in the vicinity of a metallic part is obtained from $\vec{A}$ by solving Eq. (7) simultaneously in the part and in a proper domain of air containing both the coil and the part. This impedance can be calculated by assimilating the system to a transformer.

In the case of an ECT sensor, the electrical equivalent circuit of the coil coupled to the interface of tested specimen can be represented as shown in Fig.1. The stationary coil is assumed to have a resistance R_c and inductance L_c. Similarly, the inductance and resistance of the EC path in the plate are designated by L_p and R_p, respectively. The equivalent impedance of the circuit as seen across the terminals of the stationary coil can be represented under the following form:

$$Z_{eq} = R_{eq} + jL_{eq} \quad (8)$$

where the equivalent resistance, R_{eq}, and inductance, L_{eq}, are obtained respectively as [7]

$$R_{eq} = R_c + \frac{M^2 R_p \omega^2}{R_p^2 + L_p^2 \omega^2}, \quad L_{eq} = \omega L_c - \frac{L_p M^2 R_p \omega^2}{R_p^2 + L_p^2 \omega^2} \quad (9)$$

where M is the mutual inductance between the stationary coil and the plate to be checked with EC.

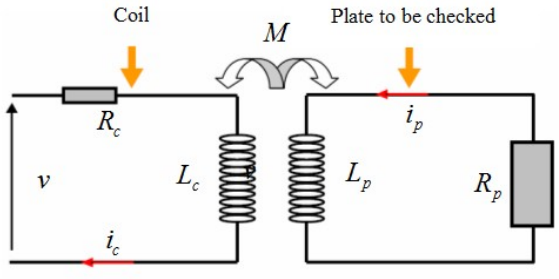

Fig. 1. Schematic of the equivalent electrical circuit of the interacting coil and inspected metallic plate.

Fig. 2 shows a double acting EC sensor for which the excitation coil serves also as a measuring element. The principle of operation of this sensor is based on the measurement of the equivalent impedance of the coil in its environment. For this, the work frequency should remain constant and the probe should be maintained at constant distance from the inspected part surface.

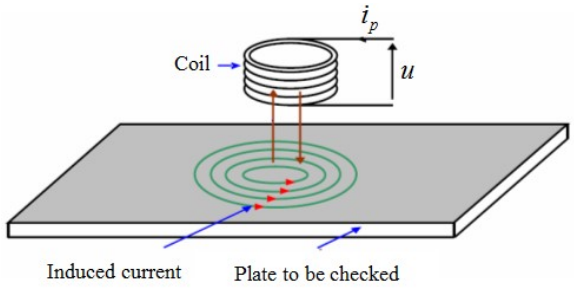

Fig.2. Phenomenological model of a double effect EC sensor.

As the presence of flaws modifies the parameters R_p, L_p and M, following-up Z_{eq} according to a B-scan procedure provides information on the existence of the flaws. Note that the equivalent impedance constitutes a better indicator than the resistance or the inductance taken alone, because it integrates also the mutual inductance. Resolution is then expected to be higher.

An essential issue to deal in the framework of ECT is how to improve the quality of sensed impedance [8]. Many parameters affect the actual value of this signal. These include the geometry of the probe. For a given frequency of work and fixed lift-off distance from the metallic part, varying the shape of the probe can yield significant variations of the obtained equivalent impedance and influences its sensitivity to some existing defects.

In this work, various probe geometries having all the same volume were studied. Fig. 3 shows the shapes that were considered. The numerical approach based on the finite element analysis was used to perform simulations. A 3-D FE model was developed for each case by means of Comsol Multiphysics software. Simulations were performed and the results analyzed using appropriate modules of this software.

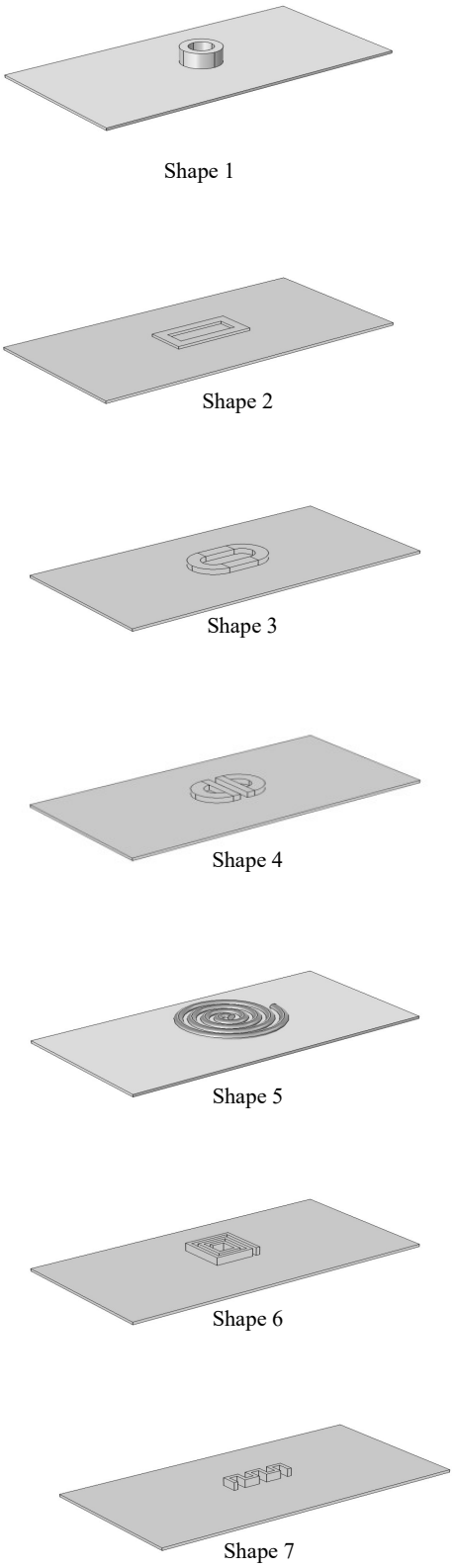

Fig. 3. Selected shapes of sensors modelled using Comsol Multiphysics software.

3 Results and discussion

In the following an aluminium rectangular plate having the dimensions (length $L_p = 800mm$, width $\ell_p = 400mm$ and thickness $h_p = 10mm$) is studied, see Fig. 4. The material of this plate has the conductivity $\sigma = 37.74 MS.m^{-1}$ and the relative permeability $\mu_r = 1H.m^{-1}$. To simulate a defect, an open cavity is implemented at the material surface at the centre of the plate. It has sides that are parallel to those of the plate with the dimensions (length $L_c = 20mm$, width $\ell_c = 20mm$ and thickness $h_c = 5mm$).

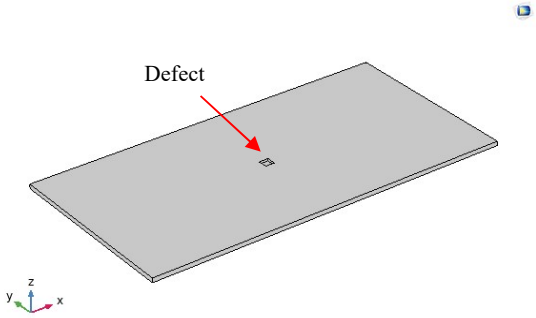

Fig. 4. Geometry of the tested plate sample

The inductive coils shown in Fig. 3 are assumed to be made of copper with electrical conductivity $\sigma' = 60 MS.m^{-1}$ and relative permeability $\mu_r' = 1H.m^{-1}$. The volumes of these coils are fixed at $V = 100mm^3$. These coils are supposed to be formed of 1000 spirals. They are assumed to be the siege of a harmonic electric current having the amplitude $I_c = 1A$. In order to have a good penetration depth, the work frequency was fixed at $f = 100Hz$. The probe was positioned at the constant distance $d = 5mm$ from the plate upper surface which is here perfectly flat. A B-scan parallel to the length of the plate was executed and five different positions of the probe were considered.

In FEM modelling, internal boundary conditions were prescribed as electric and magnetic surfaces. Also a vanishing density of charge was applied.

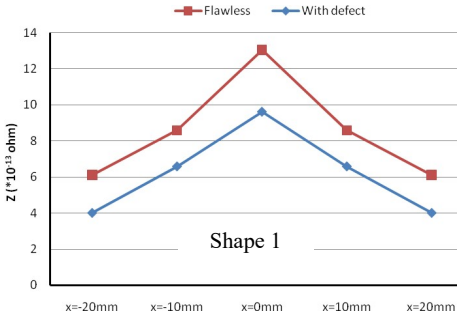

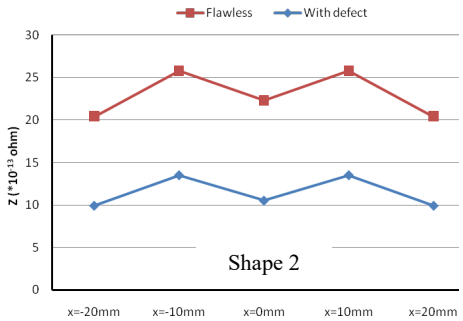

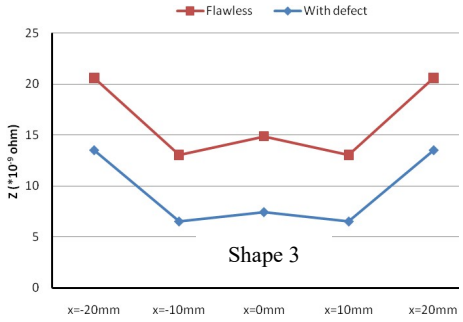

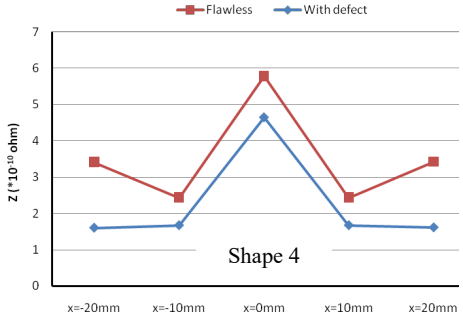

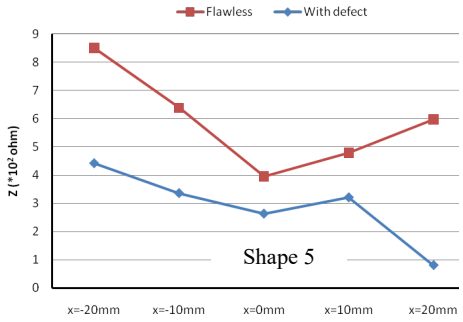

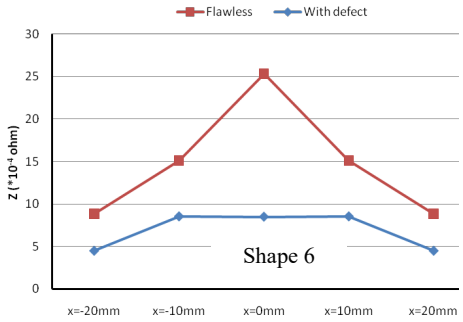

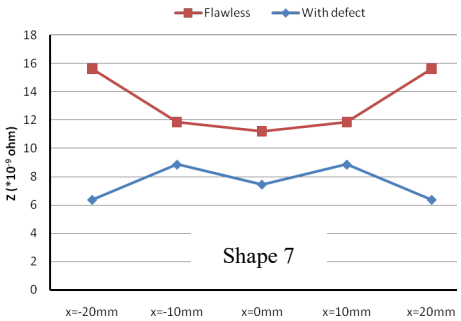

Fig. 5. Impedance of receiver coil associated to the free defect case and the defected plate for different coil shapes.

Fig. 5 gives, respectively for the seven sensors presented in Fig. 3, and the two cases of defect-free plate and flawed plate, the calculated impedance versus the relative position of the exploration sensor to the defect. Fig. 5 shows that the defect has a definite signature affecting the impedance of the coil. This can be monitored in order to sense the defect through further synthesising a proper defect indicator.

4 Conclusions

In this paper, different shapes of a transmitter/receiver EC probe have been analyzed in order to achieve defect detection in perfectly conductive parts. Simulation of these ECT devices was performed by means of Comsol Multiphysics software. For the particular case of B-scan inspection procedure, the calculated equivalent impedance was shown to undergo variations while passing above a defected zone of the part surface with a given signature. Very encouraging results have been obtained regarding the adaptation of probe shape for the purpose of increasing resolution of signature. This study opens the way to improve reliability of ECT through shaping more adequately the sensing probe.

References

1. A. Aoukili, A. Khamlichi, MATEC Web of Conferences **191**, 00003 (2018)
2. G. Cerro, L. Ferrigno, M. Laracca , F. Milano, P. Carbone, A. Comuniello, A. De Angelis, A. Moschitta, Measurement **139** (2019)
3. G. Betta, L. Ferrigno, M. Laracca, A. Rasile, S. Sangiovanni, Measurement **181** (2021)
4. G. Tytko, Bull. Pol. Ac. Tech. **68**, 6 (2020)
5. F. Jerrold, *Classical electromagnetism, second edition* (Dover Publications, Inc., New York, 2017)
6. A.A. Rodríguez, A. Valli, *Eddy Current Approximation of Maxwell Equations: theory, algorithms and applications* (Springer-Verlag, Italy, 2010)
7. N. Bowler, *Eddy-Current Nondestructive Evaluation* (Springer, New York, 2019)
8. S. She, Y. Chen, Y. He, Z. Zhou, X. Zou, Measurement **168** (2021)